

# Markov Neural Operators for Learning Chaotic Systems

Zongyi Li\*, Nikola Kovachki\*, Kamyar Azizzadenesheli†, Burigede Liu\*,  
Kaushik Bhattacharya\*, Andrew Stuart\*, Anima Anandkumar\*

June 15, 2021

## Abstract

Chaotic systems are notoriously challenging to predict because of their instability. Small errors accumulate in the simulation of each time step, resulting in completely different trajectories. However, the trajectories of many prominent chaotic systems live in a low-dimensional subspace (attractor). If the system is Markovian, the attractor is uniquely determined by the Markov operator that maps the evolution of infinitesimal time steps. This makes it possible to predict the behavior of the chaotic system by learning the Markov operator even if we cannot predict the exact trajectory. Recently, a new framework for learning resolution-invariant solution operators for PDEs was proposed, known as neural operators. In this work, we train a Markov neural operator (MNO) with only the local one-step evolution information. We then compose the learned operator to obtain the global attractor and invariant measure. Such a Markov neural operator forms a discrete semigroup and we empirically observe that does not collapse or blow up. Experiments show neural operators are more accurate and stable compared to previous methods on chaotic systems such as the Kuramoto-Sivashinsky and Navier-Stokes equations.

## 1 Introduction

**Chaotic systems.** One day in the winter of 1961, meteorologist Edward Lorenz was simulating simplified ordinary differential equations of weather using his primitive computer. Lorenz wanted to examine one particular time sequence. Instead of running the equation from the beginning, he hand-typed the initial condition from an earlier printout, and walked down the hall for a cup of coffee. When he came back, to his surprise, the result was completely different from the previous run. In the beginning, Lorenz assumed a vacuum tube had gone bad on his computer. But later, he realized that it is the seemingly negligible round-off error in the initial condition that he typed that made the simulation completely different [1]. The phenomena, also popularly known as the butterfly effect, led to the creation of chaos theory. Chaotic systems are characterized by strong instability. A tiny perturbation in the initial condition leads to a completely different trajectory. Such instability makes chaotic systems intricate and challenging both numerically and mathematically.

**Machine learning methods for chaotic systems.** Because of the intrinsic instability, it is infeasible for any method to capture the exact trajectory for a long period in a chaotic system. The correlation over a longer time is chaotic and unstable. If one tries to fit to standard ML model such as a recurrent neural network (RNN) directly on the long-time sequences, the gradient will easily blow up. Therefore, prior works either fit RNNs on very short sequences, or only learn a step-wise projection from a randomly generated evolution using reservoir computing (RC) [2–5]. These previous attempts are able to push the limit of faithful prediction to a moderate period on lower dimension systems such as ODEs like the Lorenz system or one-dimensional PDEs like the Kuramoto-Sivashinsky (KS) equation. However, they are not capable of modeling more complicated systems such as the Navier-Stokes equation (NS) which exhibits turbulence. Another approach to solving the

---

\*Caltech, {zongyili, nkovachki, bgl, bhattacharya, astuart, anima}@caltech.edu

†Purdue University, kamyar@purdue.edu

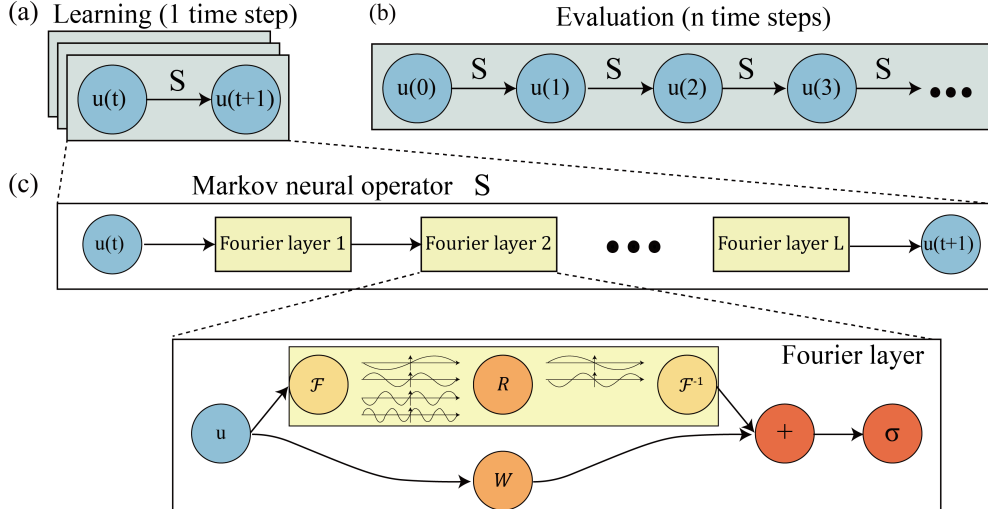


Figure 1: Markov neural operator (MNO): learn global dynamics from local data  
(a) Learn the MNO from the local time-evolution data. (b) Compose MNO to evaluate the long-time dynamic. (c) Architecture of the MNO.

chaotic PDEs is to use the equation instead of data, by using methods such as PINNs [6–8]. They are also only capable of solving, for example the KS equation, for a very short period. These results suggest that predicting long-time trajectories of such chaotic systems is, in some sense, an ill-posed problem. Instead, we take a new perspective: we predict long-time trajectories that, while eventually diverging from the truth, still preserve on the same orbit (attractor) of the system and its statistical properties.

**Invariants in chaos.** Despite the instability, many chaotic systems exhibit certain reproducible statistical properties, such as in the energy spectrum and auto-correlation, that remain the same in different realizations [1]. For instance, this holds for popular PDE families such as the KS equation and the two-dimensional NS equation (Kolmogorov flows) [9]. Mathematically, this behavior can be characterized by the existence of an invariant measure. For Markovian systems, samples from this measure can be obtained through access to a **Markov operator**, a memoryless deterministic operator that captures the evolution of the dynamics from one time step to the next. In this case, the Markov operator forms a discrete semigroup, defined by the compositions of Markov operators [10]. By learning the Markov operator, we are able to generate the attractor and estimate the invariant measure for a variety of chaotic systems that are of interest to the physics and applied mathematics communities [11–16].

**Neural operators.** To learn the Markov operators, we need to model the time-evolution of functions in infinite-dimensional function spaces. It is especially challenging when we generate long-term trajectories. Even a very small error will accumulate along the composition, potentially causing exponential build up. If one cannot capture the Markov operator with respect to the true invariant measure, the trajectories will eventually blow up or collapse. Therefore, we propose to use a recent advance in the operator-learning known as the neural operator [17]. The neural operator remedies the mesh-dependent nature of finite-dimensional operator methods such as the standard models such as RNN, RC, and CNN, and therefore better captures the invariant measure for chaotic systems.

## 1.1 Our Contributions

In this work, we exploit the ergodicity and Markovian property of the target dynamical systems. We learn a Markov neural operator (MNO) given only one-step evolution data and compose it over a long time horizon to obtain the global attractor of the chaotic system, as shown in Figure 1. The MNO forms a discrete semigroup defined by the composition of operators, allowing us to reach any state further in the future [18]. The goal is

to predict the global attractor which qualitatively does not collapse or blow up over a long or infinite time horizon, and quantitatively, shares the same distribution and statistics as the true function space trajectories.

- We learn a Markov neural operator (MNO) and compose it over a long time horizon to obtain the global attractor. Experiments show the learned Markov operator is stable and captures the long-time trajectory without collapsing or blowing up for complicated chaotic PDEs such as KS and NS.
- We show that neural operators quantitatively outperform various RNN and CNN models. Our model is 4-times more accurate for a single-step prediction and has one order of magnitude lower error on invariant statistics.
- We develop an approximation theorem that guarantees MNO is expressive enough for any locally Lipschitz system (this includes the KS and NS equations) for any finite period.
- We use Sobolev norms in operator learning. Experiments show the Sobolev norm significantly outperforms standard loss functions in preserving invariant statistics such as the spectrum.

**Invariant statistics.** We use MNO to capture invariant statistics such as the Fourier spectrum, the spectrum of the proper orthogonal decomposition (POD), the point-wise distribution, the auto-correlation, and other domain-specific statistics such as turbulence kinetic energy and dissipation rate. These invariant statistics can usually be classified as a combination of different orders of derivatives and moments. If one uses a standard mean square error (MSE) for training, the model is not able to capture the higher frequency information induced from the derivatives. Therefore, we use the Sobolev norm to address higher-order derivatives and moments [19, 20]. This is similar in spirit to pre-multiplying the spectrum by the wavenumber, an approach commonly used in fluid analysis [21]. When used for training, the Sobolev norm yields a significant improvement in capturing high frequency details compared to the standard MSE or  $L^2$  loss, and therefore we obtain a Markov operator that is able to better characterize the invariant measure.

## 2 Problem setting

We will consider infinite dimensional dynamical systems where the phase space  $\mathcal{U}$  is a Banach space and, in particular, a function space on a Lipschitz domain  $D \subset \mathbb{R}^d$ . We are interested in the initial-value problem

$$\begin{aligned} \frac{du}{dt}(t) &= F(u(t)), & t \in (0, \infty), \\ u(0) &= u_0, \end{aligned} \tag{1}$$

for initial conditions  $u_0 \in \mathcal{U}$  where  $F$  is usually a non-linear operator. We will assume, given some appropriate boundary conditions on  $\partial D$ , that the solution  $u(t) \in \mathcal{U}$  exists and is unique for all times  $t \in (0, \infty)$ . When making the spatial dependence explicit, we will write  $u(x, t)$  to indicate the evaluation  $u(t)|_x$  for any  $x \in D$ . We adapt the viewpoint of casting time-dependent PDEs into function space ODEs (1), as this leads to the semigroup approach to evolutionary PDEs which underlies our learning methodology.

### 2.1 Markov operators and the semigroup

Since the Banach-valued ODE (1) is autonomous, that is,  $F$  does not explicitly depend on time, under the well-posedness assumption, we may define, for any  $t \in [0, \infty)$ , a Markov operator  $S_t : \mathcal{U} \rightarrow \mathcal{U}$  such that  $u(t) = S_t u(0)$ . This map satisfies the properties

1.  $S_0 = I$ ,
2.  $S_t(u_0) = u(t)$ ,
3.  $S_t(S_s(u_0)) = u(t + s)$ ,

for any  $s, t \in [0, \infty)$  and any  $u_0 \in \mathcal{U}$  where  $I$  denotes the identity operator on  $\mathcal{U}$ . In particular, the family  $\{S_t : t \in [0, \infty)\}$  defines a semigroup of operators acting on  $\mathcal{U}$ . Our goal is to approximate a particular element of this semigroup associated to some fixed time step  $h > 0$  given observations of the trajectory from (1). We build an approximation  $\hat{S}_h : \mathcal{U} \rightarrow \mathcal{U}$  such that

$$\hat{S}_h \approx S_h \tag{2}$$

**Long-term predictions.** Note that having access to the map  $\hat{S}_h$  from (2) allows for approximating long time trajectories of (1) by repeatedly composing  $\hat{S}_h$  with its own output. Indeed, by (2) and the semigroup property, we find that

$$u(n \cdot h) \approx \hat{S}_h^n(u_0) := \underbrace{(\hat{S}_h \circ \dots \circ \hat{S}_h)}_{n \text{ times}}(u_0) \tag{3}$$

for any  $n \in \mathbb{N}$ . This fact is formalized in Theorem 1 which is stated in the proceeding section. It is important to note that the approximation from (3) is  $n$ -dependent, in particular, predicting a trajectory well is only possible up to a finite time (unless there is some special feature in the dynamic such as periodicity). Luckily, for many practical applications, it is not necessary to predict exact trajectories of a system. Rather, it is sufficient to characterize statistical properties of the system's long time behavior. This is especially true for chaotic systems where very small perturbations can result in large long time deviations. Many such systems occur in nature, for example, in the turbulent flow of fluids. In the current work, we take the perspective of accurately characterizing such statistical properties.

## 2.2 Attractors, ergodicity, and invariant measures.

**Global Attractors.** The long time behavior of the solution to (1) is characterized by the set  $U = U(u_0) \subset \mathcal{U}$  which is invariant under the dynamic i.e.  $S_t(U) = U$  for all  $t \geq 0$ , and the orbit  $u(t)$  converges

$$\inf_{v \in U} \|u(t) - v\|_{\mathcal{U}} \rightarrow 0 \quad \text{as} \quad t \rightarrow \infty.$$

When it exists,  $U$  is often identified as the  $\omega$ -limit set of  $u_0$ . The chaotic nature of certain dynamical systems arises due to the complex structure of this set because  $u(t)$  follows  $U$  and  $U$  can be, for example, a fractal set. For dissipative systems, such sets exist and constitute a larger, **global attractor**  $\mathcal{A} \subset \mathcal{U}$  which is compact and attracts all orbits  $u(t)$ , in particular,  $\mathcal{A}$  is independent of the initial condition  $u_0$ . Many PDEs arising in physics such as reaction-diffusion equations describing chemical dynamics or the Navier-Stokes equation describing the flow of fluids are dissipative and possess a global attractor which is often times finite-dimensional [9]. Therefore, numerically characterizing the attractor is an important problem in scientific computing with many potential applications.

**Data distribution.** For many applications, an exact form for the possible initial conditions to (1) is not available; it is therefore convenient to use a stochastic model to describe the initial states. To that end, let  $\mu_0$  be a probability measure on  $\mathcal{U}$  and assume that all possible initial conditions to (1) come as samples from  $\mu_0$  i.e.  $u_0 \sim \mu_0$ . Then any possible state of the dynamic (1) after some time  $t > 0$  can be thought of as being distributed according to the pushforward measure  $\mu_t := S_t^\# \mu_0$  i.e.  $u(t) \sim \mu_t$ . Therefore as the dynamic evolves, so does the type of likely functions that result. This further complicates the problem of long time predictions since training data may only be obtained up to finite time horizons hence the model will need the ability to predict not only on data that is out-of-sample but also out-of-distribution.

**Ergodic systems.** To alleviate some of the previously presented challenges, we consider **ergodic** systems. Roughly speaking, a system is ergodic if there exists an **invariant measure**  $\mu$  such that after some  $T > 0$ , we have  $\mu_t \approx \mu$  for any  $t \geq T$  (in fact,  $\mu$  can be defined without any reference to  $\mu_0$  or its pushforwards, see [22] for details). That is, after some large enough time, the distribution of possible states that the system can be in is fixed for any time further into the future. Indeed,  $\mu$  charges the global attractor  $\mathcal{A}$ . Notice that ergodicity is a much more general property than having **stationary states** which means that the system has a fixed period in time, or having **steady states** which means the system is unchanged in time.

Ergodicity mitigates learning a model that is able to predict out-of-distribution since both the input and the output of  $\hat{S}_h$  will approximately be distributed according to  $\mu$ . Furthermore, we may use  $\hat{S}_h$  to learn about  $\mu$  since sampling it simply corresponds to running the dynamic forward. Indeed, we need only generate data on a finite time horizon in order to learn  $\hat{S}_h$ , and, once learned, we may use it to sample  $\mu$  indefinitely by simply repeatedly composing  $\hat{S}_h$  with itself. Having samples of  $\mu$  then allows us to compute statistics which characterize the long term behavior of the system and therefore the global attractor  $\mathcal{A}$ . Note further that this strategy avoids the issue of accumulating errors in long term trajectory predictions since we are only interested in the property that  $\hat{S}_h(u(t)) \sim \mu$ .

**Remark.** Notably, the existence of a global attractor does not imply the existence of an invariant measure. Indeed, the only deterministic and chaotic systems that are proven to possess an invariant measure are certain ODEs such as the Lorenz-63 system [23]. On the other hand, proving the existence of an invariant measure for deterministic and chaotic PDEs such as the KS or NS equations are still open problems, despite ergodic behavior being observed empirically.

### 3 Markov neural operator

We propose the Markov neural operator, a method for learning the underlying Markov operators of chaotic dynamical systems. In particular, we approximate the operator mapping the solution from the current step to the next step  $\hat{S}_h : u(t) \mapsto u(t+h)$ . The architecture of the Markov neural operator is detailed in Figure 1. Markov neural operators employs a local transformation  $P$  to lift the input function  $u(t) \in \mathcal{U}$  to a higher dimensional representation  $v_0(x) = P(u(x, t))$ . We model this step using a fully-connected neural network. The lifting step provides a rich representation for later steps of the Markov neural operator. The computation of  $v_0$  is followed by multiple layers of iterative updates  $v_l \mapsto v_{l+1}$  which consist of applying non-linear operators formed by the composition of a non-local integral operator  $K_{\phi_l}$  with a non-linear activation function  $\sigma$ . That is

$$v_{l+1}(x) := \sigma\left(Wv_l(x) + (K_{\phi_l}v_l)(x)\right), \quad \forall x \in D \quad (4)$$

where  $K_{\phi_l} : \mathcal{U} \rightarrow \mathcal{U}$  is a linear operator parameterized by  $\phi_l \in \Theta_l$  a finite-dimensional space. The operator  $K_{\phi_l}$  is chosen to be a kernel integral operator parameterized by a neural network,

$$(K_{\phi_l}v_l)(x) := \int_D \kappa_{\phi_l}(x, y)v_l(y)dy, \quad \forall x \in D \quad (5)$$

where the kernel function  $\kappa_{\phi_l} : \mathbb{R}^{2d} \rightarrow \mathbb{R}^{d_v \times d_v}$  is a neural network parameterized by  $\phi_l$ . Finally, the output  $u(x, t+h) \approx Q(v_L(x))$  is the projection of  $v_L$  by the local transformation  $Q : \mathbb{R}^{d_v} \rightarrow \mathbb{R}^{d_u}$  which is again given by a fully-connected neural network. The work Li et al. [24] proposes the Fourier neural operator (FNO) as an efficient implementation of neural operators by assuming  $\kappa_{\phi_l}(x, y) = \kappa_{\phi_l}(x - y)$ . In this case, (5) is a convolution operator. FNO exploits the structure of convolution by parameterizing  $\kappa_{\phi_l}$  directly in Fourier space and using the Fast Fourier Transform (FFT) to efficiently compute (5), in particular,

$$(K_{\phi_l})(x) = \mathcal{F}^{-1}\left(R_{\phi_l} \cdot (\mathcal{F}v_l)\right)(x) \quad \forall x \in D \quad (6)$$

where  $R_{\phi_l}$  is the Fourier transform of a periodic function  $\kappa_l : D \rightarrow \mathbb{R}^{d_v \times d_v}$  parameterized directly by the Fourier coefficients  $\phi_l \in \Theta_l$  and  $\mathcal{F}$  is the FFT. This leads to a fast architecture that obtains state-of-the-art results for certain PDE problems. In this paper, we adopt this implementation of neural operators to design the Markov neural operator.

Having adopted the neural operator parametric class, we prove the following theorem regarding the Markov neural operator. The result states that our construction can approximate trajectories of infinite-dimensional dynamical systems arbitrary well. The proof is given in the Appendix.

**Theorem 1.** *Let  $K \subset \mathcal{U}$  be a compact set and assume that, for some  $h > 0$ , the Markov operator  $S_h : \mathcal{U} \rightarrow \mathcal{U}$  associated to the dynamic (1) is locally Lipschitz. Then, for any  $n \in \mathbb{N}$  and  $\epsilon > 0$  there exists a neural*

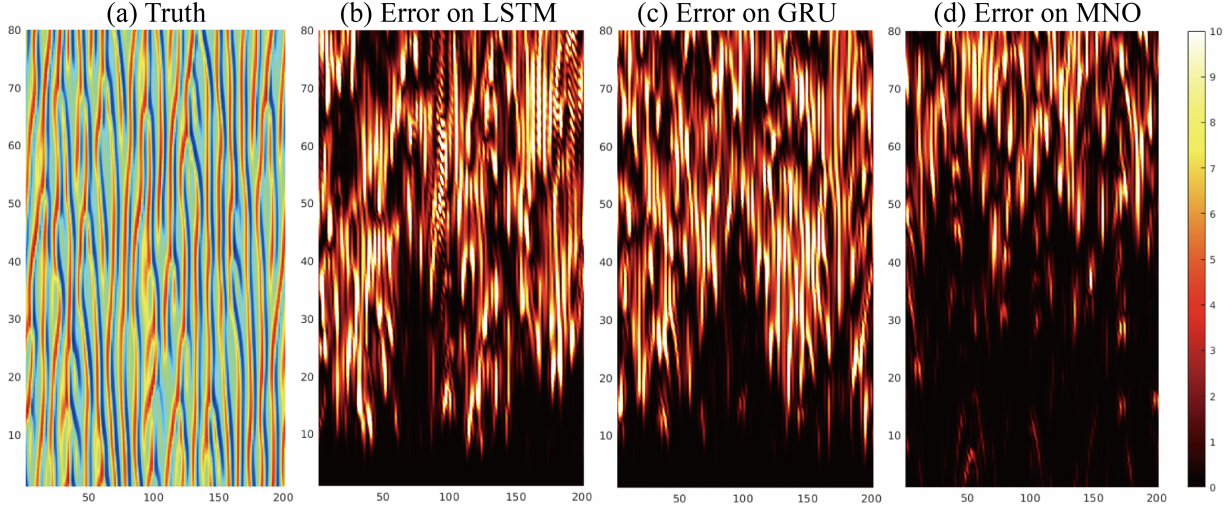


Figure 2: Trajectory and error on the KS equation

The x-axis is the spatial domain; the y-axis is the temporal domain. The figure shows that LSTM and GRU start to diverge at  $t = 20s$  while MNO is able to keep up with the exact trajectory until  $t = 50s$ .

operator  $\hat{S}_h : \mathcal{U} \rightarrow \mathcal{U}$  such that

$$\sup_{u_0 \in K} \sup_{k \in \{1, \dots, n\}} \|u(kh) - \hat{S}_h^k(u_0)\|_{\mathcal{U}} < \epsilon.$$

Theorem 1 indicates that the class of MNOs is rich enough to approximate many chaotic dynamical systems for a arbitrarily long period. Standard neural network such as RNNs and CNNs do not possess such approximation theorems that hold in the infinite-dimensional setting. Furthermore we expect that it is possible to show that the global attractor can be approximated arbitrarily well by adapting ideas from the standard theory of numerical integrators such as [25].

## 4 Experiments

In this section, we present the experiment for the Kuramoto-Sivashinsky equation and the Kolmogorov flow raising from the 2-d Navier-Stokes equation. Both PDEs exhibit chaotic behavior.

### 4.1 Kuramoto-Sivashinsky equation

We consider the following one-dimensional Kuramoto-Sivashinsky equation,

$$\begin{aligned} \frac{\partial u}{\partial t} &= -u \frac{\partial u}{\partial x} - \frac{\partial^2 u}{\partial x^2} - \frac{\partial^4 u}{\partial x^4}, & \text{on } [0, L] \times (0, \infty) \\ u(\cdot, 0) &= u_0, & \text{on } [0, L] \end{aligned} \quad (7)$$

where  $L = 32\pi$  or  $64\pi$  and the spatial domain  $[0, L]$  is equipped with periodic boundary conditions. We assume the initial condition  $u_0 \in \dot{L}_{\text{per}}^2([0, L]; \mathbb{R})$ , where  $\dot{L}_{\text{per}}^2([0, L]; \mathbb{R})$  is the space of all mean zero  $L^2$ -functions that are periodic on  $[0, L]$ . Existence of the semigroup  $S_t : \dot{L}_{\text{per}}^2([0, L]; \mathbb{R}) \rightarrow \dot{L}_{\text{per}}^2([0, L]; \mathbb{R})$  is established in [9, Theorem 3.1]. Data is obtained by solving the equation using the exponential time-differencing fourth-order Runge-Kutta method from [26]. Random initial conditions are generated according to a mean zero Gaussian measure with covariance  $L^{-2/\alpha} \tau^{\frac{1}{2}(2\alpha-1)} (-\Delta + (\tau^2/L^2)I)^{-\alpha}$  where  $\alpha = 2$ ,  $\tau = 7$ , and periodic boundary conditions on  $[0, L]$ ; for details see [27].

**Benchmarks for Kuramoto-Sivashinsky.** We compare MNO with common choices of recurrent neural networks including the long short-term memory network (LSTM)[28] and gated recurrent unit (GRU)[29]. All models use the time-discretization  $h = 1s$ . The training dataset consists of 1000 different realizations of trajectories on the time interval  $t \in [50, 200]$  (the first 50s is truncated so the dynamics reach the ergodic state), which adds up to  $1000 \times 150 = 150,000$  snapshots in total. Another 200 realizations are generated for testing. Every single snapshot has the resolution 2048. We use Adam optimizer to minimize the relative  $L^2$  loss with learning rate  $= 0.001$ , and step learning rate scheduler that decays by half every 10 epochs for 50 epochs in total. **LSTM and GRU:** having tested many different configurations, we choose the best hyper-parameters: the number of layers  $= 1$ , width  $= 1000$ . During the evaluation, we additionally provide 1000 snapshots as a warm-up of the memory. **MNO:** we choose 1-d Fourier neural operator as our base model with four Fourier layers with 20 frequencies per channel and width  $= 64$ . Experiments run on Nvidia V100 GPUs.

**Accuracy with respect to the true trajectory.** In general, MNO has a smaller per-step error compared to RNN. As shown in Figure 2, the MNO model captures a longer period of the exact trajectory compared to LSTM and GRU. LSTM and GRU start to diverge at  $t = 20s$  while FNO is able to keep up with the exact trajectory until  $t = 50s$ .

**Invariant statistics for the KS equations** As shown in Figure 3, we present enormous invariant statistics for the KS equation. We use 150000 snapshots to train the MNO, LSTM, and GRU to model the evolution operator of the KS equation with  $h = 1s$ . We compose each model for  $T = 1000$  time steps to obtain a long trajectory (attractor), and estimate various invariant statistics from them.

- **(a) Fourier spectrum:** the Fourier spectrum of the predicted attractor. All models are able to capture the Fourier modes with magnitude larger than  $O(1)$ , while MNO is more accurate on the tail.
- **(b) Spatial correlation:** the spatial correlation of the attractor, averaged in the time dimension. MNO is more accurate on the near-range correlation, but all models miss the long-range correlation.
- **(c) Auto-correlation of the Fourier mode:** the auto-correlation of the  $10^{th}$  Fourier mode. Since the Fourier modes are nearly constant, the auto-correlation is constant too.
- **(d) Auto-correlation of the PCA mode:** the auto-correlation of the first PCA mode (with respect to the PCA basis of the ground truth data). The PCA mode oscillates around  $[-40, 40]$ , showing an ergodic state.
- **(e) Distribution of kinetic energy:** the distribution of kinetic energy with respect to the time dimension. MNO captures the distribution most accurately.
- **(f) Pixelwise distribution of velocity:** since the KS equation is homogeneous, we can compute the distribution of velocity with respect to pixels. MNO captures the pixelwise distribution most accurately too.

**Choice of time discretization.** We further study the choice of time steps  $h$ . As shown in Figure 4, when the time steps are too large, the correlation is chaotic and hard to capture. But counter-intuitively, when the time steps are too small, the evolution is also hard to capture. In this case, the input and output of the network will be very close, and the identity map will be a local minimum. An easy fix is to use MNO to learn the time-derivative or residual. This is shown in the figure, where the residual model (blue line) has a better per-step error and accumulated error at smaller  $h$ . When the time step is large, there is no difference in modeling the residual. This idea can generalize to other integrators as an extension of Neural ODEs to PDEs [30].

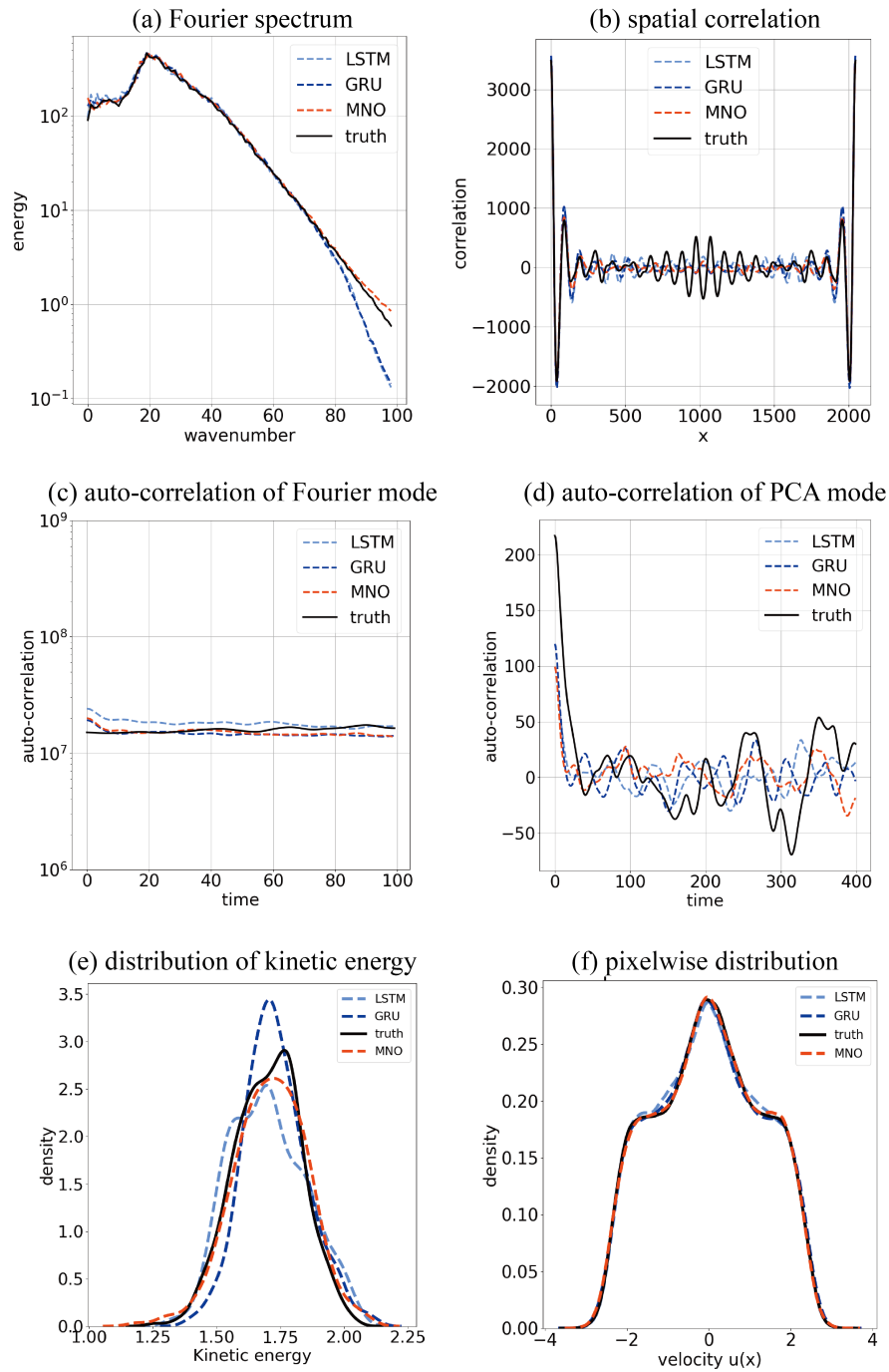


Figure 3: Invariant statistics for the KS equation



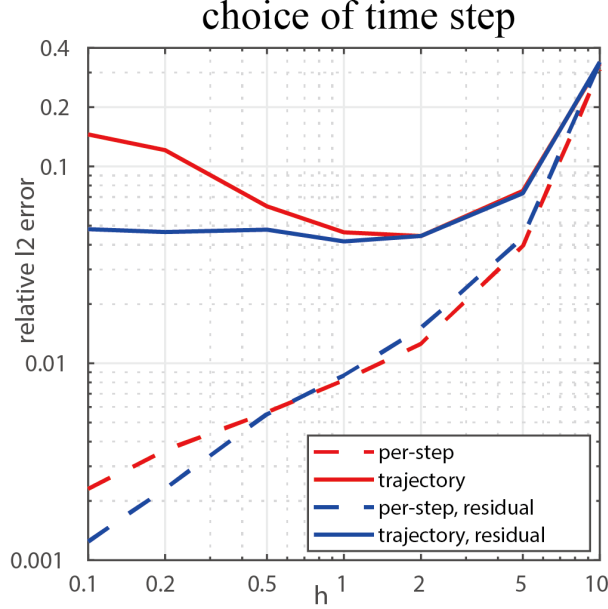


Figure 4: Choice of time step.

## 4.2 Navier-Stokes equation

We consider the two-dimensional Navier-Stokes equation for a viscous, incompressible fluid,

$$\begin{aligned}
 \frac{\partial u}{\partial t} &= -u \cdot \nabla u - \nabla p + \frac{1}{Re} \Delta u + \sin(ny)\hat{x}, & \text{on } [0, 2\pi]^2 \times (0, \infty) \\
 \nabla \cdot u &= 0 & \text{on } [0, 2\pi]^2 \times [0, \infty) \\
 u(\cdot, 0) &= u_0 & \text{on } [0, 2\pi]^2
 \end{aligned} \tag{8}$$

where  $u$  denotes the velocity,  $p$  the pressure, and  $Re > 0$  is the Reynolds number. The domain  $[0, 2\pi]^2$  is equipped with periodic boundary conditions. The specific choice of forcing  $\sin(ny)\hat{x}$  constitutes a Kolmogorov flow; we choose  $n = 4$  in all experiments. We define  $\mathcal{U}$  to be the closed subspace of  $L^2([0, 2\pi]^2; \mathbb{R}^2)$ ,  $\mathcal{U} = \{u \in \dot{L}^2_{\text{per}}([0, 2\pi]^2; \mathbb{R}^2) : \nabla \cdot u = 0\}$  and assume  $u_0 \in \mathcal{U}$ . We define the vorticity  $w = (\nabla \times u)\hat{z}$  and the stream function  $f$  as the solution to the Poisson equation  $-\Delta f = w$ . Existence of the semigroup  $S_t : \mathcal{U} \rightarrow \mathcal{U}$  is established in [9, Theorem 2.1]. We denote turbulence kinetic energy (TKE)  $\langle (u - \bar{u})^2 \rangle$ , and dissipation  $\epsilon = \langle w^2 \rangle / Re$ . Data is obtained by solving the equation in vorticity form using the pseudo-spectral split step method from [13]. Random initial conditions are generated according to a mean zero Gaussian measure with covariance  $7^{3/2}(-\Delta + 49I)^{-2.5}$  with periodic boundary conditions on  $[0, 2\pi]^2$ .

**Benchmarks for 2d Navier-Stokes.** We compare MNO with common standard two-dimensional dynamic models including U-Net[31] and LSTM-CNN[32] on modeling the vorticity  $w$ . We choose the discretization  $h = 1s$ . The training dataset consists of 180 realizations of trajectories on time interval  $t \in [100, 500]$  (the first 100 seconds are discarded) which adds up to  $180 \times 400 = 72,000$  snapshots in total. Another 20 realizations are generated for testing. Each single snapshot has resolution  $64 \times 64$ . We use the Adam optimizer to minimize the relative  $L^2$  loss with learning rate = 0.0005, and step learning rate scheduler that decays by half every 10 epochs for 50 epochs in total. **U-Net:** we use five layers of convolution and deconvolution with width from 64 to 1024. **LSTM-CNN:** we use one layer of LSTM with width = 64. **MNO:** we parameterize the 2-d Fourier neural operator consists of four Fourier layers with 20 frequencies per channel and width = 64.

**Accuracy with respect to various norms.** MNO shows near one order of magnitude better accuracy compared to U-Net and LSTM-CNN. As shown in Table 1, we train each model using the balanced  $L^2 (= H^0)$ ,

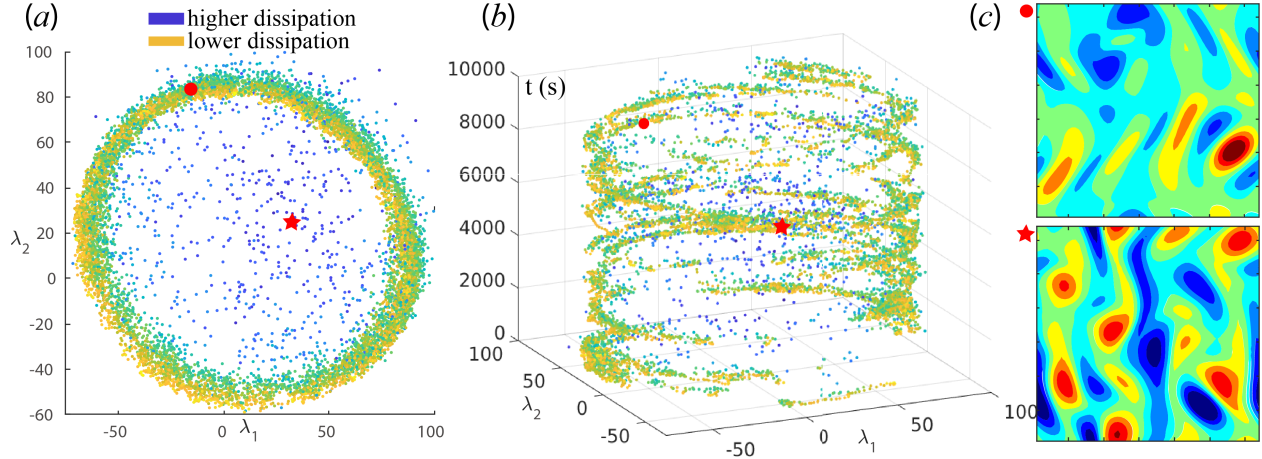


Figure 5: The learned attractor of the Kolmogorov flow.

The 10000 time steps trajectory generated by MNO projected onto the first two components of PCA. Each point corresponds to an snapshot on the attractor. Two points are selected for further visualization of vorticity field.

Model	training	loss	$L^2$ error	$H^1$ error	$H^2$ error	TKE error	$\epsilon$ error
MNO	$L^2$ loss	0.0166	0.0187	0.0474	0.1729	<b>0.0136</b>	0.0303
	$H^1$ loss	0.0184	0.0151	0.0264	0.0656	0.0256	<b>0.0017</b>
	$H^2$ loss	0.0202	<b>0.0143</b>	<b>0.0206</b>	<b>0.0361</b>	0.0226	0.0193
U-Net	$L^2$ loss	0.0269	0.0549	0.1023	0.3055	0.0958	0.0934
	$H^1$ loss	0.0377	0.0570	0.0901	0.2164	0.1688	0.1127
	$H^2$ loss	0.0565	0.0676	0.0936	0.1749	0.0482	0.0841
ConvLSTM	$L^2$ loss	0.2436	0.2537	0.3854	1.0130	0.0140	24.1119
	$H^1$ loss	0.2855	0.2577	0.3308	0.5336	0.6977	6.9167
	$H^2$ loss	0.3367	0.2727	0.3311	0.4352	0.8594	4.0976

Table 1: Benchmark on vorticity for the Kolmogorov flow with  $Re=40$

$H^1$ , and  $H^2$  losses, defined as the sum of the relative  $L^2$  loss grouped by each order of derivative. And we measure the error with respect to the standard (unbalanced) norms. The MNO with  $H^2$  loss consistently achieves the smallest error on vorticity on all of the  $L^2$ ,  $H^1$ , and  $H^2$  norms. However,  $L^2$  loss achieves the smallest error on the turbulence kinetic energy (TKE);  $H^1$  loss achieves the smallest error on the dissipation  $\epsilon$ .

The NS equation with  $Re=40$  is shown in Figure 6. (a) show the ground truth data of vorticity field, each column represents a snapshot at  $t = 100s$  with a different initial condition. (b), (c), (d) show the predicted trajectory of MNO on vorticity, using  $L^2$ ,  $H^1$ , and  $H^2$  losses respectively. We are able to generate a long trajectory with the MNO model. The five columns represent  $t = 1000s, 2000s, 3000s, 4000s, 5000s$  respectively. As shown in the figure, the predicted trajectories (b) (c) (d) share the same behaviors as in the ground truth (a). It indicates the MNO model is stable.

**Visualizing the attractor generated by MNO.** We compose MNO 10000 times to obtain the global attractor, and we compute the PCA (POD) basis of these 10000 snapshots and project them onto the first two components. As shown in Figure (a), we obtain a cycle-shaped attractor. The true attractor has a degree of freedom around  $O(100)$  [9]. If the attractor is a high-dimensional sphere, then most of the mass concentrates around its equator. Therefore, when projected to low-dimension, the attractor will have the shape of a ring. Most of the points are located on the ring, while a few other points are located in the center.

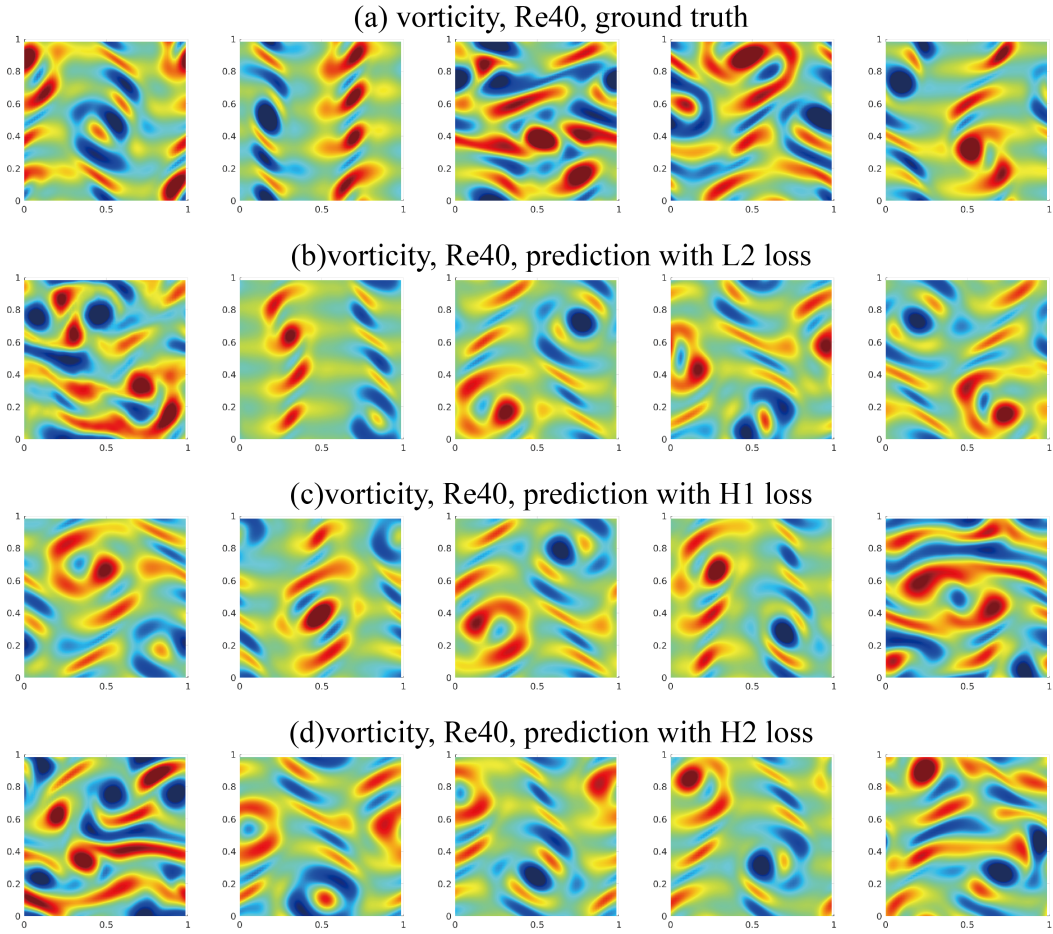


Figure 6: visualization of the NS equation, Re40

The points in the center have high dissipation, implying they are intermittent states. In Figure (b) we add the time axis. While the trajectory jumps around the cycle, we observe there is a rough period of 2000s. We perform the same PCA analysis on the training data, which shows the same behavior.

**Invariant statistics.** Similarly, we present enormous invariant statistics for the NS equation (Re40), as shown in Figure 7. We use 72000 snapshots to train the MNO, UNet, and ConvLSTM to model the evolution operator of the KS equation with  $h = 1s$ . We compose each model for  $T = 10000$  time steps to obtain a long trajectory (attractor), and estimate various invariant statistics from them.

- **(a, d) Fourier spectrum of velocity and vorticity:** the Fourier spectrum of the predicted attractor. Again, all models are able to capture the Fourier modes with magnitude larger than  $O(1)$ , while MNO is more accurate on the tail. Using the Sobolev norm further helps to capture the tail.
- **(b, e) Pixelwise distribution of velocity and vorticity:** All models preserve the pixelwise distribution.
- **(c, f) Distribution of kinetic energy and dissipation rate:** the distribution of kinetic energy with respect to the time dimension. MNO captures the distribution most accurately.
- **(g) Auto-correlation of the Fourier mode:** the auto-correlation of the 10<sup>th</sup> Fourier mode. Since the Fourier modes are nearly constant, the auto-correlation is constant too. Notice it is very expensive to generate long-time ground truth data, so the figure does not include the ground truth. However, it is easy to obtain the auto-correlation by MNO.
- **(h) Auto-correlation of the PCA mode:** the auto-correlation of the first PCA mode (with respect to the PCA basis of the ground truth data). The PCA mode oscillates around  $[-1000, 1000]$ , showing an ergodic state. The UNet oscillates around  $[0, 2000]$ .
- **(i) Spatial correlation:** the spatial correlation of the attractor, averaged in the time dimension. The four columns represent the truth and MNO with different losses. As seen from the figure, there is a wave pattern matching the force term  $\sin(4y)$ .

**Order of derivatives.** Roughly speaking, vorticity is the derivative of velocity; velocity is the derivative of the stream function. Therefore we can denote the order of derivative of vorticity, velocity, and stream function as 2, 1, and 0 respectively. Combining vorticity, velocity, and stream function, with  $L^2$ ,  $H^1$ , and  $H^2$  loss, we have in total the order of derivatives ranging from 0 to 4. We observe, in general, it is best practice to keep the order of derivatives in the model at a number slightly higher than that of the target quantity. For example, as shown in Figure 8, when querying the velocity (first-order quantity), it is best to use second-order (modeling velocity plus  $H^1$  loss or modeling vorticity plus  $L^2$  loss). This is further illustrated in Table 2. In general, using a higher order of derivatives as the loss will increase the power of the model and capture the invariant statistics more accurately. However, a higher-order of derivative means higher irregularity. It in turn requires a higher resolution for the model to resolve and for computing the discrete Fourier transform. This trade-off again suggests it is best to pick a Sobolev norm not too low or too high.

## 5 Discussion and future work

In this work, we learn MNO from only local data and compose it to obtain the global attractor of chaotic systems. The MNO forms a discrete semigroup defined by the composition of operators that empirically does not collapse or blow up over a long or infinite time horizon. Experiments also show MNO predicts the attractor that shares the same distribution and statistics as the true function space trajectories. The Markov operator and chaotic systems are mathematically interesting and physically relevant. MNO shows potential for application studying the bifurcation of complicated system, for example, in the modeling of chemical reactions and the flow of turbulent fluids.

This work provides a method for fast computation in many scientific computing problems. These methods have two main long-term impacts beyond the immediate interests of scientific computing communities.

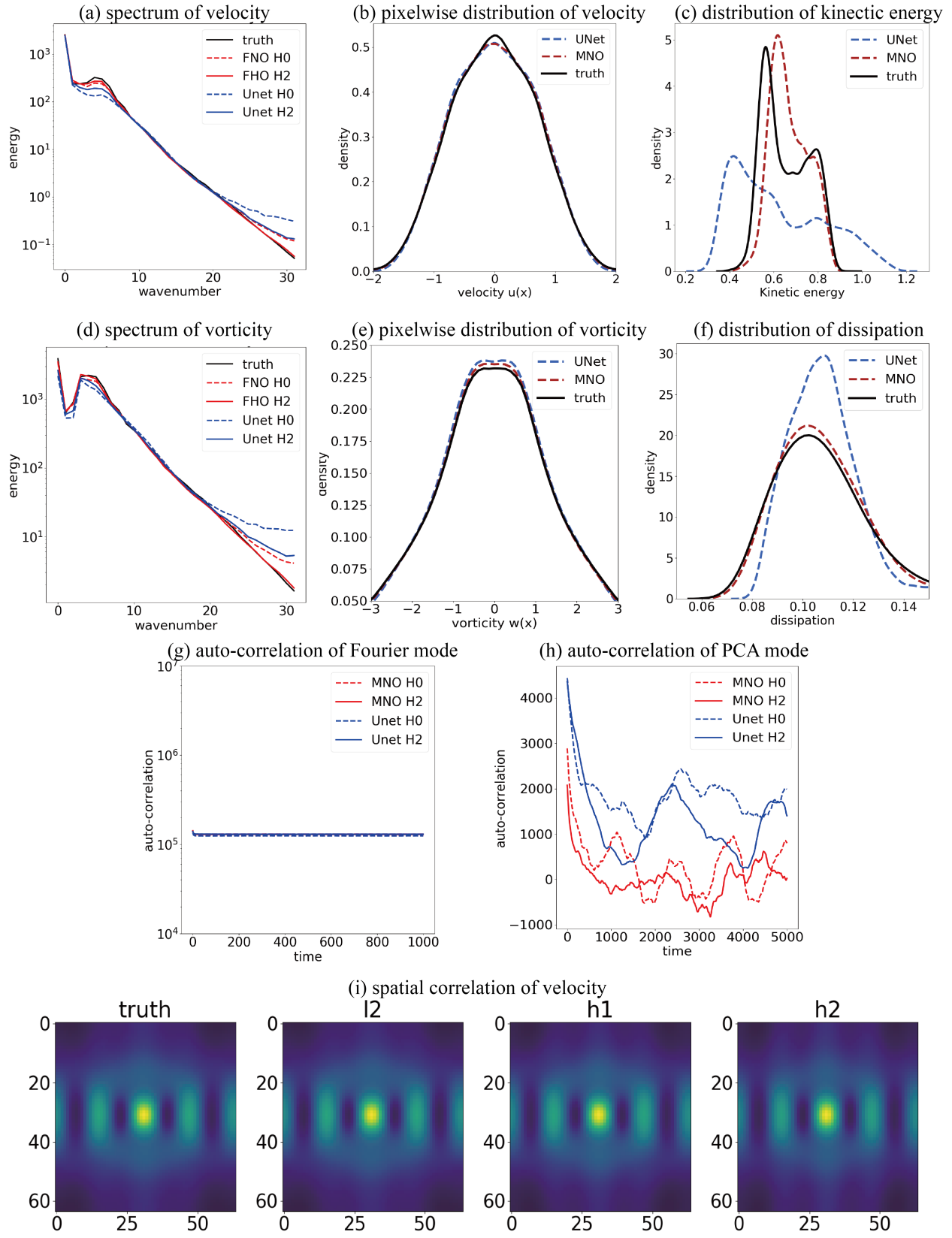


Figure 7: Invariant statistics for the NS equation

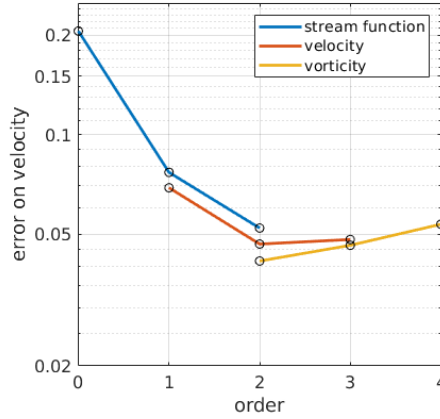


Figure 8: Error on velocity with respect to the order of derivative.

Model	training loss	(order)	error on $f$	error on $u$	error on $w$
Stream function $f$	$L^2$ loss	0.0379 (0 <sup>th</sup> order)	0.0383	0.2057	2.0154
Stream function $f$	$H^1$ loss	0.0512 (1 <sup>st</sup> order)	0.0268	0.0769	0.3656
Stream function $f$	$H^2$ loss	0.0973 (2 <sup>nd</sup> order)	0.0198	0.0522	0.2227
Velocity $u$	$L^2$ loss	0.0688 (1 <sup>st</sup> order)	0.0217	0.0691	0.3217
Velocity $u$	$H^1$ loss	0.1246 (2 <sup>nd</sup> order)	<b>0.0170</b>	0.0467	0.1972
Velocity $u$	$H^2$ loss	0.2662 (3 <sup>rd</sup> order)	0.0178	0.0482	0.1852
Vorticity $w$	$L^2$ loss	0.1710 (2 <sup>nd</sup> order)	0.0219	<b>0.0415</b>	0.1736
Vorticity $w$	$H^1$ loss	0.3383 (3 <sup>rd</sup> order)	0.0268	0.0463	<b>0.1694</b>
Vorticity $w$	$H^2$ loss	0.4590 (4 <sup>th</sup> order)	0.0312	0.0536	0.1854

Table 2: Vorticity, velocity, and stream function for the Kolmogorov flow with  $Re = 500$

Since our methods are orders of magnitude faster than traditional solvers that are prominently used in supercomputers, edge devices, and servers, the deployment of our methods significantly reduces the carbon footprints caused by scientific studies. Furthermore, the proposed methods are extremely flexible. The off the shelf usage of our methods allows scientists from a variety of disciplines, from chemistry, biology, ecology, epidemiology, to physics and applied mathematics to deploy our methods to their complex PDE of interest (or any other problem that involves learning maps between function spaces).

MNO has two major limitations. First, it assumes the target system is approximately Markovian. If the system is heavily path-dependent, then the MNO framework does not directly apply. Second, although we develop an approximation theorem for finite period, it does not hold for infinite time horizon.

As discussed previously, it is infeasible to track the exact trajectory of chaotic systems on an infinite time horizon. Even very small errors will accumulate in each step, and eventually cause the simulation to diverge from the true trajectory. However, it is possible to track the attractor of the system. An attractor is absorbing. If the simulated trajectory only makes a small error, the attractor will absorb it back, so that the simulated trajectory will never diverge from the true attractor. Therefore, it is possible to have the simulated trajectory capture the true attractor.

To obtain an infinite-time approximation error bound is non-trivial. Previously, [10, 33] (cf. Theorem 3.12) show a result for (finite-dimensional) ODE systems. If the system is Lipschitz then there exists a numerical simulation that forms a dissipative dynamical system that does not blow up or collapse. And the the simulated attractor  $\mathcal{A}_h$  approximates the true attractor  $\mathcal{A}$  with the time step  $h$

$$\text{dist}(\mathcal{A}_h, \mathcal{A}) \rightarrow 0, \quad \text{as } h \rightarrow 0$$

To generalize such theorem to Markov neural operator (MNO), we need to overcome two difficulties (1)

generalize the formulation from (finite-dimensional) ODE systems to (infinite-dimensional) PDE systems, and (2) show MNO can obtain a sufficient error rate with respect to the time step  $h$ .

The first aspect requires extending the theory from finite dimension to infinite dimension, which is non-trivial since the operator  $F$  in (1) is not compact or bounded. This makes it hard to bound the error with respect to the attractor [34]. The second aspect requires to formulate MNO slightly differently. In the current formulation, the evolution operator is chosen for a fixed time step  $h$ . To achieve  $O(h)$  error we need to formulate the evolution operator continuously for infinitesimal  $h$ . Especially, for a semi-linear PDE system

$$\frac{du}{dt} + Au = F(u)$$

where  $A$  is a linear, self-adjoint operator and  $F$  is a continuous but nonlinear operator (This formulation includes the KS and NS equations). The evolution can be written as

$$u(t+h) = e^{-Ah}u(t) + \int_0^h e^{-A(h-s)}F(u(t+s))ds$$

Where  $\Phi(u(t), A, t) := \int_0^h e^{-A(h-s)}F(u(s))ds$  is bounded despite  $F$  is not. If one can approximate  $\Phi(u(t), A, h)$  by a neural operator, then MNO can potentially achieve the needed error rate. This shows hope to obtain an approximation error bound for infinite time zero. We leave this as a promising future direction.

## Acknowledgements

Z. Li gratefully acknowledges the financial support from the Kortschak Scholars Program. A. Anandkumar is supported in part by Bren endowed chair, LwLL grants, Beyond Limits, Raytheon, Microsoft, Google, Adobe faculty fellowships, and DE Logi grant. K. Bhattacharya, N. B. Kovachki, B. Liu, and A. M. Stuart gratefully acknowledge the financial support of the Army Research Laboratory through the Cooperative Agreement Number W911NF-12-0022. Research was sponsored by the Army Research Laboratory and was accomplished under Cooperative Agreement Number W911NF-12-2-0022. The views and conclusions contained in this document are those of the authors and should not be interpreted as representing the official policies, either expressed or implied, of the Army Research Laboratory or the U.S. Government. The U.S. Government is authorized to reproduce and distribute reprints for Government purposes notwithstanding any copyright notation herein.

## References

- [1] James Gleick. *Chaos: Making a new science*. Open Road Media, 2011.
- [2] Pantelis R Vlachas, Wonmin Byeon, Zhong Y Wan, Themistoklis P Sapsis, and Petros Koumoutsakos. Data-driven forecasting of high-dimensional chaotic systems with long short-term memory networks. *Proceedings of the Royal Society A: Mathematical, Physical and Engineering Sciences*, 474(2213):20170844, 2018.
- [3] Jaideep Pathak, Brian Hunt, Michelle Girvan, Zhixin Lu, and Edward Ott. Model-free prediction of large spatiotemporally chaotic systems from data: A reservoir computing approach. *Physical review letters*, 120(2):024102, 2018.
- [4] Pantelis R Vlachas, Jaideep Pathak, Brian R Hunt, Themistoklis P Sapsis, Michelle Girvan, Edward Ott, and Petros Koumoutsakos. Backpropagation algorithms and reservoir computing in recurrent neural networks for the forecasting of complex spatiotemporal dynamics. *Neural Networks*, 2020.
- [5] Huawei Fan, Junjie Jiang, Chun Zhang, Xingang Wang, and Ying-Cheng Lai. Long-term prediction of chaotic systems with machine learning. *Physical Review Research*, 2(1):012080, 2020.
- [6] Maziar Raissi. Deep hidden physics models: Deep learning of nonlinear partial differential equations. *The Journal of Machine Learning Research*, 19(1):932–955, 2018.

- [7] Nicholas Geneva and Nicholas Zabaras. Modeling the dynamics of pde systems with physics-constrained deep auto-regressive networks. *Journal of Computational Physics*, 403:109056, 2020.
- [8] Yohai Bar-Sinai, Stephan Hoyer, Jason Hickey, and Michael P Brenner. Learning data-driven discretizations for partial differential equations. *Proceedings of the National Academy of Sciences*, 116(31):15344–15349, 2019.
- [9] Roger Temam. *Infinite-dimensional dynamical systems in mechanics and physics*, volume 68. Springer Science & Business Media, 2012.
- [10] A. Stuart and A.R. Humphries. *Dynamical Systems and Numerical Analysis*. Cambridge Monographs on Applie. Cambridge University Press, 1998. ISBN 9780521645638.
- [11] Kai Fukami, Koji Fukagata, and Kunihiko Taira. Machine-learning-based spatio-temporal super resolution reconstruction of turbulent flows. *Journal of Fluid Mechanics*, 909, 2021.
- [12] José I Cardesa, Alberto Vela-Martín, and Javier Jiménez. The turbulent cascade in five dimensions. *Science*, 357(6353):782–784, 2017.
- [13] Gary J Chandler and Rich R Kerswell. Invariant recurrent solutions embedded in a turbulent two-dimensional kolmogorov flow. *Journal of Fluid Mechanics*, 722:554–595, 2013.
- [14] Péter Koltai and Stephan Weiss. Diffusion maps embedding and transition matrix analysis of the large-scale flow structure in turbulent rayleigh–bénard convection. *Nonlinearity*, 33(4):1723, 2020.
- [15] Jason J Bramburger, J Nathan Kutz, and Steven L Brunton. Data-driven stabilization of periodic orbits. *IEEE Access*, 9:43504–43521, 2021.
- [16] Jacob Page, Michael P Brenner, and Rich R Kerswell. Revealing the state space of turbulence using machine learning. *Physical Review Fluids*, 6(3):034402, 2021.
- [17] Zongyi Li, Nikola Kovachki, Kamyar Azizzadenesheli, Burigede Liu, Kaushik Bhattacharya, Andrew Stuart, and Anima Anandkumar. Neural operator: Graph kernel network for partial differential equations. *arXiv preprint arXiv:2003.03485*, 2020.
- [18] Georgy Anatolevich Sviridyuk. On the general theory of operator semigroups. *Russian Mathematical Surveys*, 49(4):45–74, 1994.
- [19] Wojciech Marian Czarnecki, Simon Osindero, Max Jaderberg, Grzegorz Świrszcz, and Razvan Pascanu. Sobolev training for neural networks. *arXiv preprint arXiv:1706.04859*, 2017.
- [20] Alex Beatson, Jordan Ash, Geoffrey Roeder, Tianju Xue, and Ryan P Adams. Learning composable energy surrogates for pde order reduction. *Advances in Neural Information Processing Systems*, 33, 2020.
- [21] Alexander J Smits, Beverley J McKeon, and Ivan Marusic. High–reynolds number wall turbulence. *Annual Review of Fluid Mechanics*, 43:353–375, 2011.
- [22] Grigorios Pavliotis and Andrew Stuart. *Multiscale Methods: Averaging and Homogenization*, volume 53. 01 2008. ISBN 978-0-387-73828-4. doi: 10.1007/978-0-387-73829-1.
- [23] Mark Holland and Ian Melbourne. Central limit theorems and invariance principles for Lorenz attractors. *Journal of the London Mathematical Society*, 76(2):345–364, 10 2007.
- [24] Zongyi Li, Nikola Kovachki, Kamyar Azizzadenesheli, Burigede Liu, Kaushik Bhattacharya, Andrew Stuart, and Anima Anandkumar. Fourier neural operator for parametric partial differential equations. *arXiv preprint arXiv:2010.08895*, 2020.
- [25] A. R. Humphries and A. M. Stuart. Runge–kutta methods for dissipative and gradient dynamical systems. *SIAM Journal on Numerical Analysis*, 31(5):1452–1485, 1994.



- [26] Aly-Khan Kassam and Lloyd N. Trefethen. Fourth-order time-stepping for stiff pdes. *SIAM Journal on Scientific Computing*, 26(4):1214–1233, 2005.
- [27] Gabriel J Lord, Catherine E Powell, and Tony Shardlow. *An introduction to computational stochastic PDEs*, volume 50. Cambridge University Press, 2014.
- [28] Felix A Gers, Jürgen Schmidhuber, and Fred Cummins. Learning to forget: Continual prediction with lstm. 1999.
- [29] Junyoung Chung, Caglar Gulcehre, KyungHyun Cho, and Yoshua Bengio. Empirical evaluation of gated recurrent neural networks on sequence modeling. *arXiv preprint arXiv:1412.3555*, 2014.
- [30] Tian Qi Chen, Yulia Rubanova, Jesse Bettencourt, and David K Duvenaud. Neural ordinary differential equations. In *Advances in neural information processing systems*, pages 6571–6583, 2018.
- [31] Olaf Ronneberger, Philipp Fischer, and Thomas Brox. U-net: Convolutional networks for biomedical image segmentation. In *International Conference on Medical image computing and computer-assisted intervention*, pages 234–241. Springer, 2015.
- [32] Xingjian Shi, Zhourong Chen, Hao Wang, Dit-Yan Yeung, Wai-Kin Wong, and Wang-chun Woo. Convolutional lstm network: A machine learning approach for precipitation nowcasting. *arXiv preprint arXiv:1506.04214*, 2015.
- [33] AR Humphries and AM Stuart. Runge–kutta methods for dissipative and gradient dynamical systems. *SIAM journal on numerical analysis*, 31(5):1452–1485, 1994.
- [34] Andrew Stuart. *Perturbation theory for infinite dimensional dynamical systems*. 1995.
- [35] Nikola B. Kovachki, Zongyi Li, Liu Burigede, Kamyar Azizzadenesheli, Kaushik Bhattacharya, Andrew M. Stuart, and Anima Anandkumar. Neural operator: Learning maps between function spaces. *In Preparation*.

## 6 Appendix

### 6.1 Proof of Theorem 1

*Proof of Theorem 1.* Since  $S_h$  is continuous and  $K$  is compact, the set

$$R = \bigcup_{l=0}^n S_h^l(K)$$

is compact. Therefore, there exist a set of representers  $\varphi_1, \varphi_2, \dots \in R$  such that

$$\lim_{m \rightarrow \infty} \sup_{v \in R} \inf_{u \in R_m} \|u - v\|_{\mathcal{U}} = 0$$

where  $R_m = \text{span}\{\varphi_1, \dots, \varphi_m\}$ . For any  $m \in \mathbb{N}$ , let  $P_m : \mathcal{U} \rightarrow R_m$  denote a projection of  $U$  to  $R_m$ . Since  $R$  is compact, the set

$$P = R \bigcup \left( \bigcup_{m=1}^{\infty} P_m(R) \right)$$

is compact. Since  $S_h$  is locally Lipschitz and  $P$  is compact, there exists a constant  $C = C(P) > 0$  such that

$$\|S_h(u_1) - S_h(u_2)\|_{\mathcal{U}} \leq C \|u_1 - u_2\|_{\mathcal{U}}, \quad \forall u_1, u_2 \in P.$$

Without loss of generality, assume  $C \neq 1$  and define

$$M = \left( C^n + \frac{1 - C^n}{1 - C} \right)^{-1}.$$

By the universal approximation theorem for neural operators [35], there exists a neural operator  $\hat{S}_h : \mathcal{U} \rightarrow \mathcal{U}$  such that

$$\sup_{u_0 \in P} \|S_h(u_0) - \hat{S}_h(u_0)\|_{\mathcal{U}} < \epsilon M.$$

Perusal of the proof of the universal approximation theorem for neural operators shows that  $\hat{S}_h$  can be chosen so that  $\hat{S}_h(P) \subseteq R_m$  for some  $m \in \mathbb{N}$  large enough, therefore  $\hat{S}_h(P) \subseteq P$ . Let  $u_0 \in K$ , then the triangle inequality implies

$$\begin{aligned} \|u(nh) - \hat{S}_h^n(u_0)\|_{\mathcal{U}} &= \|S_h^n(u_0) - \hat{S}_h^n(u_0)\|_{\mathcal{U}} \\ &= \|S_h(S_h^{n-1}(u_0)) - \hat{S}_h(\hat{S}_h^{n-1}(u_0))\|_{\mathcal{U}} \\ &\leq \|S_h(S_h^{n-1}(u_0)) - S_h(\hat{S}_h^{n-1}(u_0))\|_{\mathcal{U}} + \|S_h(\hat{S}_h^{n-1}(u_0)) - \hat{S}_h(\hat{S}_h^{n-1}(u_0))\|_{\mathcal{U}} \\ &\leq C \|S_h^{n-1}(u_0) - \hat{S}_h^{n-1}(u_0)\|_{\mathcal{U}} + \epsilon M. \end{aligned}$$

By the discrete time Grönwall lemma,

$$\begin{aligned} \|u(nh) - \hat{S}_h^n(u_0)\|_{\mathcal{U}} &\leq C^n \|S_h(u_0) - \hat{S}_h(u_0)\|_{\mathcal{U}} + \epsilon M \left( \frac{1 - C^n}{1 - C} \right) \\ &< \epsilon M \left( C^n + \frac{1 - C^n}{1 - C} \right) \\ &= \epsilon \end{aligned}$$

which completes the proof. □